UDC 537.9 DOI: 10.15222/TKEA2018.5-6.10

A. F. BELYANIN[1], V. V. BORISOV[2], V. V. POPOV[3]

Russia, Moscow, [1]Central Research Technological Institute "Technomash",
[2]Skobeltsyn Institute of Nuclear Physics of Lomonosov Moscow State University,
[3]Lomonosov Moscow State University

E-mail: belyanin@cnititm.ru

X-RAY RADIATION DURING PULSED LASER TREATMENT OF OPAL MATRICES

The paper presents the structure and preparation conditions of opal matrices (ordered 3D-lattice packing of X-ray amorphous SiO_2 spheres with a diameter of ≈250 nm), as well as experimental data on nonlinear optical effects in opal matrices with pulsed laser excitation at wavelengths: 1040 nm, 510 nm in conjunction with 578 nm, and 366 nm. The authors investigate the energy spectra of X-ray radiation induced in the samples by laser irradiation.

Keywords: opal matrix, laser radiation, X-ray radiation, energy spectrum.

Materials with photonic band gaps (photonic crystals), i. e. materials with a periodic (of the order of the light wavelength) change in the dielectric constant, are currently the subject of extensive theoretical and experimental research. Photonic crystals based on opal matrices **(OM)** are of interest for practical application. OMs are made up of well ordered closely packed silica nanospheres (amorphous SiO_2) of the same diameter [1, 2]. The packing of spheres contains a 3D system of interconnecting octahedral and tetrahedral inter-sphere voids, occupying approximately 26% of the matrix volume. Depending on the formation conditions, the diameter of the spheres varies within the preassigned limits from 200 to 700 nm [2–5].

Having the formation parameters fixed, the variation in diameter does not exceed 1.5%. OMs and OM-based nanocomposites (OMs with intersphere voids filled with various substances) are used to create devices operating in the optical, microwave and THz ranges [3, 6]. OMs may serve as functional environments both for the generation of X-rays or acoustic waves, and for signal conversion in controlling devices [7, 8]. One may hope that the emergence of new designs using such materials will allow creating electronic devices with improved performance characteristics.

The greatest interest is aroused by the application of OMs in an unexplored area of the X-ray generation by exposing the substance to laser radiation [7, 9]. Solving the problem of increasing the technical and technological characteristics of X-ray sources by creating fundamentally new designs can lead to the development of subminiature X-ray sources. Coupling laser radiation into optical fibers is widely used to solve a large number of practical problems, for example, it is used in medicine for endoscopic studies of internal organs, pyrometry, spectroscopy, etc. Placing the OM at the output of the optical fiber with laser radiation makes it possible to deliver X-ray radiation directly to the irradiated object.

When a parallel fiber is added to transmit data to a Raman spectrometer, it becomes possible to monitor the effectiveness of local X-ray influence. When solving a large number of practical problems, such as transporting radiation to an object of impact in medicine, etc., a high-power laser can be coupled into the optical fiber. In [7], X-ray radiation was induced when a single pulse of a ruby laser was applied to an OM (wavelength 694.3 nm, pulse duration 20 ns, maximum pulse energy 0.3 J, power density at the focus 0.25–10 GW/cm^2). X-ray radiation was registered using an X-ray film designed for a photon energy of 10 keV. This method, though, allows determining the energy characteristics of the radiation with some level of approximation.

In this study, an X-ray spectrometer is used to study the energy spectra of X-ray radiation induced by exposure of opal matrices to pulsed laser radiation with different wavelengths: 1040 nm (IR spectral range), 510 and 578 nm (combined modes), and 366 nm (UV range).

Experimental samples

Opal matrices were obtained at a temperature of 310–350 K from an emulsion prepared by mixing 1 part of a 25% aqueous solution of ammonium hydroxide (NH_4OH), 50 parts of ethanol

The study was supported by the Russian Foundation for Basic Research (grant N 18-29-02076 мк)

(C_2H_5OH) and 1.6 parts of tetraether orthosilicic acid ($Si(OC_2H_5)_4$) [10]. The regularity of the packing of SiO_2 spherical particles was achieved due to self-organization, and the diameter of the spheres depended on the conditions of their formation. The chemicals used in the preparation of OMs were removed from the samples by heat treatment in vacuum (775—975 K, ≈ 1 Pa). Then the OMs were hydrothermally hardened at increased temperature and pressure. The hardening made it possible to mechanically process the OMs, and thus obtain samples of the required dimensions with specified physical properties.

The test samples were made to be 1.5—5.0 mm thick plates obtained by dry mechanical treatment from bulk OMs, either not hardened or hardened by annealing at up to 1475 K in air. The arithmetic mean deviation of the plate surface profile, measured with an Alpha-Step 200 profilograph-profilometer, was R_a = 1.2 μm. The experiments were performed on both unfilled OMs and OMs with the inter-spherical voids filled with deionized water (OM:H_2O) to reduce the thermal effect of laser radiation. With the same purpose, a number of experiments were carried out with samples immersed in liquid nitrogen (OM:L_{N2}).

X-ray research technique

The X-radiation occurring from laser irradiation of the OM was recorded using a photographic film placed in an opaque cassette and a Canberra UniSpec 503 gamma spectrometer operating at room temperature without cooling. The data obtained from the spectrometer were calibrated by the spectra of four test X-ray sources (^{55}Fe, ^{133}Ba, ^{152}Eu and ^{241}Am isotopes).

When the radiation was registered by a film as it is shown in **Fig. 1**, the laser radiation passed through the OM and its direction coincided with the direction of the induced X-radiation (φ = 0°). The parameters of the laser radiation were chosen so that the material of the cassette (thick black paper covered with Scotch transparent adhesive film) that is not transparent to visible light would not be destroyed. The photosensitivity of the photo film (type 42) was 1000—1400 units (state standard ГОСТ 10691.5), sensitization limit 700—730 nm.

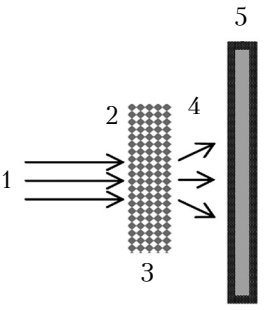

Fig. 1. Schematic illustration of registering X-radiation by photo film at φ = 0°:
1 — laser radiation; *2* — focal plane of laser radiation; *3* — OM (10×10×1.5 mm) with H_2O; *4* — X-radiation; *5* — photo film cassette

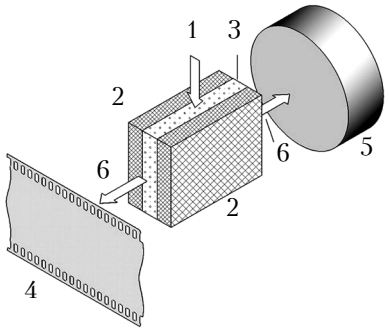

Fig. 2. Schematic illustration of registering X-ray radiation by gamma-spectrometer and photo film at φ = 90°:
1 — laser radiation; *2* — $LiNbO_3$ plates (10×10×1 mm); *3* — OM (10×10×(3—5) mm); *4* — photo film cassette; *5* — spectrometer sensor window; *6* — X-radiation

In some cases, during registration of micro X-ray radiation, laser radiation was applied to the OM placed between two plates of single crystal lithium niobate ($LiNbO_3$), a piezoelectric material [11], and X-rays were recorded at an angle of 90° to the direction of laser radiation (**Fig. 2**). This was done in order to avoid damaging the spectrometer sensor window made of beryllium foil.

The parameters of the used laser radiation sources are given in **Table 1**, where λ is the wavelength, *f* is the frequency, τ is the pulse duration, *P* is the average pulse power, *D* is the diameter of the laser beam at the focus. For systems with a galvanometric scanner of the laser beam (IR_{1040}, UV_{355}), the following areas were processed during one OM laser irradiation session: a 5×5 mm square with a 20 lines/mm linear shading on the OM focal plane when registering at an angle of 0°, and a 5 mm long line on the verge of the OM parallel to the OM focal plane when registering at an angle of 90°.

Table 1

The parameters of the used laser radiation sources

Laser radiation source, manufacturer (designation)	λ, nm	*f*, kHz	τ, ns	*P*, W	*D*, μm
YLP-1-20, IRE-POLUS (IR_{1040})	1040	50	10	10	50
DPSS UV Pro, "Sharplase" (UV_{355})	355	40	20	3	37
CVL, LPI RAS (C_{VL})	510, 578	10	15	3	20

Study of the structure and composition of opal matrices

Tests were performed on opal matrices with a volume of up to 1 cm^3, a diameter of SiO_2 spheres $d \approx 250$ nm ($\Delta d \approx 2\%$) and a volume of monodomain regions (areas of well ordered sphere packing) of at least 0.1 mm^3. The following pieces of equipment were used: a Carl Zeiss Leo 1430 VP scanning electron microscope (SEM); a JEM 200C transmission electron microscope (TEM); an ARL X'tra (Thermo Fisher Scientific) X-ray diffractometer, and a LabRAM HR800(HORIBA Jobin-Yvon) laser Raman spectrometer (632.8 nm line of He—Ne laser).

It was established that in the OM samples, the monodomain regions are disordered relative to each other (**Fig. 3**, *a*). Under the conditions assumed in this study, a three-layer (cubic) packing of SiO_2 spheres was formed [10]. The hardening of the OM was caused by the transfer of SiO_2 to the region of contact between the spheres with the formation of –Si–O–Si– bonds. Transmission electron microscopy shows the presence of contact pads with a diameter of $k = (0.1-0.3)d$ while the SiO_2 particles maintain the regular spherical shape and are not deformed at their contact points (Fig. 3, *c*). The high bond strength of the contacting SiO_2 spheres can be seen on chipped edges of the OM, where the areas of their separation are visible (Fig. 3, *b*).

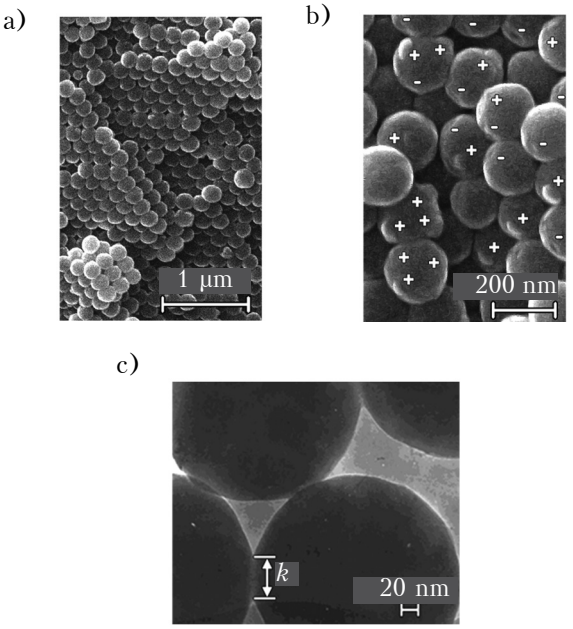

Fig. 3. SEM images of the growth surface (*a*) and chipped edge (*b*) of the OM, and a TEM image of the contact area of SiO_2 spheres (*c*)
(in *b*, pluses represent convex areas, and minuses stand for concave areas in the points where the spheres are separated between the contact pads)

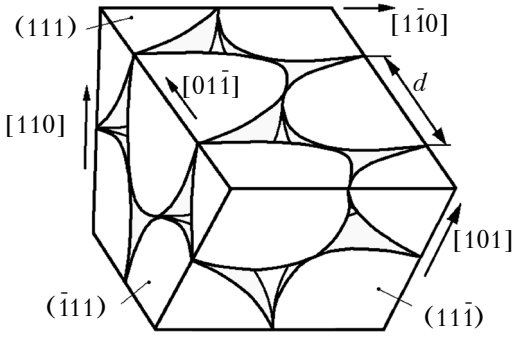

Fig. 4. Bulk fragment of the OM (cut along {111} planes)

Fig. 4 shows the bulk model of the OM (lattice packing of SiO_2 nanospheres) with the spatial ordered arrangement of inter-sphere voids. The triangles with concave sides on the cutout planes of the bulk fragment of the OM are the cross-sections of the channels, connecting the tetrahedral and octahedral inter-sphere voids. It should be noted that in hardened OMs, the real dimensions of the voids are smaller than the theoretical ones.

X-ray diffractometry revealed that the OMs, annealed in air at 1475 K, contain a phase of SiO_2 cristobalite (space group $P4_12_12$) with approximately 20-nm crystallites (areas of coherent X-rays scattering). In samples annealed at temperatures below 1475 K, it is impossible to register this phase using X-ray diffraction — the small crys-

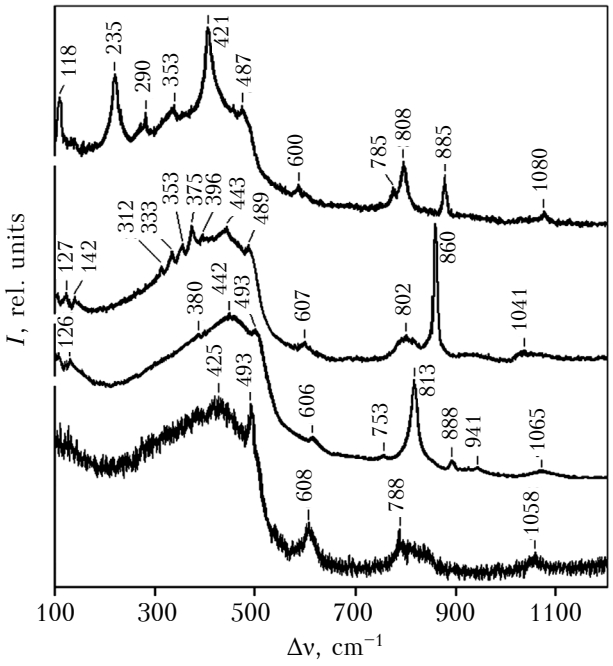

Fig. 5. Raman spectra of the OM, annealed at different temperatures and time periods:
1 — 1175 K, 4 h; *2* — 1325 K, 24 h; *3* — 1375 K, 4 h; *4* — 1475 K, 8 h

tallite size (<1 nm) does not allow identifying them due to the size broadening of the diffraction maxima, according to the Debye–Sherrer equation. In this case, the crystalline phase of SiO_2 was identified by Raman spectroscopy of Raman scattering. Raman spectra of amorphous SiO_2 are characterized by bands with a frequency shift $\Delta\nu$ of Raman scattering near 420, 490, 600, 800 and 1060 cm^{-1} (**Fig. 5**, curve *1*). At temperatures above 1175 K, amorphous silica begins recrystallizing into SiO_2-cristobalite (space group $P4_12_12$); at 1375 K, the crystalline phase of SiO_2-quartz (space group $P3_12_1$) is formed (band at $\Delta\nu = 860$ cm^{-1}), which at 1475 K is transformed into SiO_2-cristobalite (Fig. 5)

Investigation of induced pulsed X-radiation

In some cases, during measurements using the spectrometer, the speed of data acquisition in the X-ray energy range up to 2 keV depended on both environmental conditions and the power of the computing equipment used. Therefore, in order to obtain reliable results from the absolute numerical data of the X-ray spectrum (abs.), the background values of the spectrum registered when the laser source was blocked, were subtracted, thus obtaining a corrected spectrum (rel.).

The experimental conditions and the parameters of the obtained X-ray radiation are summarized in **Table 2**, where V is the scanning speed (for the systems without a C_{VL} galvanometric scanner, the laser beam is stationary); φ is the angle of X-ray registration; h_1 is the distance from the OM to the photo film cassette; h_2 is the distance from the OM to the spectrometer window; OM_{an} is the OM strengthened by annealing; S_T is the type of spectrum; t is the duration of one laser radiation session; E_{XR} is the energy of X-ray quanta corresponding to the maximum intensity peak in the spectrum; λ_{XR} is the X-ray wavelength corresponding to E_{XR}.

As can be seen from **Fig. 6** and **7**, when OMs are exposed to laser radiation with a wavelength of $\lambda = 1040$ nm, the induced X-ray radiation is scattered more strongly than at $\lambda = 355$ nm. Moreover, when exposed to laser radiation from the UV region, compared to the IR region, intense luminescence in the visible light range is observed in the hardened OM. It is possible that the high sensitivity of the used photo film causes halos to appear in the photographs (see Fig. 7), which is due to the thermal effect of laser radiation on the sample through the protective material of the cassette. The photographs

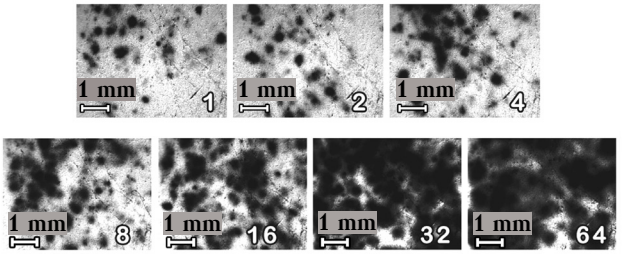

Fig. 6. Images obtained when X-ray radiation induced by the UV_{355} source was applied to the film at $\varphi = 0°$, $V = 1$ m/s (the numbers on the images are the number of repetitions of the laser radiation session)

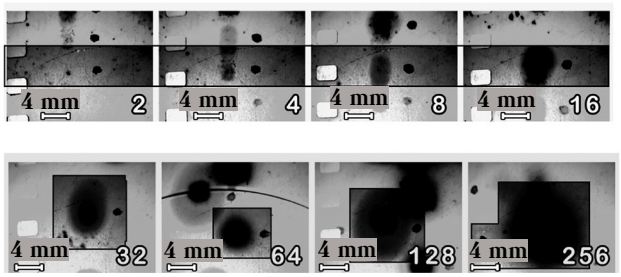

Fig. 7. Images obtained when X-ray radiation induced by an IR_{1040} source was applied to a film at $\varphi = 0°$, $V = 0.8$ m/s
(the numbers on the images are the number of repetitions of a laser radiation session; the area of X-ray radiation exposure is framed, the point of impact is marked with a dot)

Table 2

Experimental conditions and parameters of the obtained X-ray radiation

Source	V, m/s	φ, °	h_1, mm	h_2, mm	Sample		S_T	t, s	E_{XR}, keV	λ_{XR}, nm
					composition	thickness, mm				
IR_{1040}	0,8	90	2,5	2,5	$OM:H_2O$	1,5	abs.	60	0,08	15,2
UV_{355}	1,0								1,04	1,2
C_{VL}	0	90	70	80	$OM:L_{N2}$	5,0	rel.	220	1,04	1,2
		0			$OM_{an}:H_2O$	1,5		698	2,47	0,5

obtained using the UV_{355} and C_{VL} laser sources, unlike the IR_{1040}, show a domain structure of the OM (see Fig. 6 and 7) [7, 8].

The obtained data given in Table 2 and **Fig. 8**, indicate that the radiation under study is a low-intensity, soft X-ray radiation and its wavelength range intersects with the vacuum UV radiation, which is well absorbed by air. By its characteristics, it is similar to the radiation produced by triboluminescence of adhesive Scotch films at the moments when they are detached from smooth surfaces [12]. The X-ray spectrum induced by laser radiation with $\lambda = 355$ nm has an additional, shorter-wavelength peak $\lambda_{XR} = 1.2$ nm, compared to $\lambda_{XR} = 15.2$ nm on the spectrum obtained at $\lambda = 1040$ nm (see table 2). An even shorter wavelength peak ($\lambda_{XR} = 0.5$ nm) is observed when using an C_{VL} source with combined modes $\lambda = 510$ nm and $\lambda = 578$ nm (see Table 2 and Fig. 8).

Fig. 9 shows a photograph of a film after exposure to X-ray radiation induced by the C_{VL} source.

The test results for the study of dried and non-thermally hardened OMs at the wavelength of laser radiation $\lambda = 355$ nm with the parameters specified in tables 1 and 2 for the UV_{355} source, also showed the presence of X-rays. However, in contrast to OM_{an}:H_2O (strengthened OMs with voids filled with H_2O), in these samples some defects characteristic of laser ablation occurred during the course of the experiment.

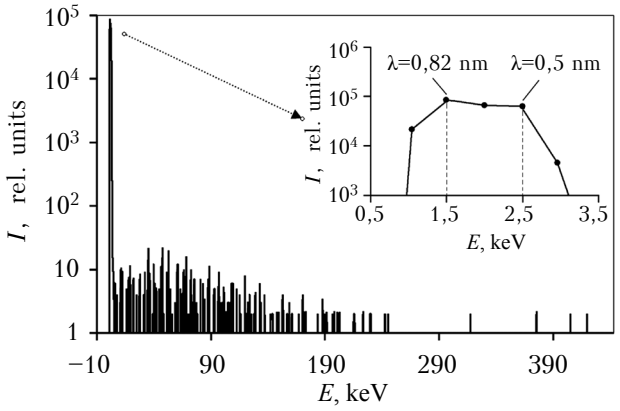

Fig. 8. Relative X-ray spectrum induced by the C_{VL} source in the OM under the following conditions: OM_{an}:H_2O thickness 1.5 mm, $\varphi = 0°$, $h_2 = 80$ mm, $E_{XR} = 2.5$ keV, $t = 698$ s, $\lambda_{XR} = 0.5$ nm (insert shows the maximum intensity spectrum peak)

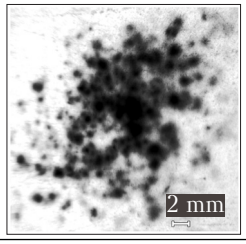

Fig. 9. Image obtained by exposing the photo film to X-ray radiation with the spectrum shown in Fig. 8 ($h_1 = 70$ mm, $t = 2$ s)

Conclusion

Thus, the studies of opal matrices indicate that the parameters of induced X-ray radiation depend on the production conditions and the structure of the OMs (high-temperature annealing, filling of voids, sample thickness), as well as the experimental conditions (obtaining of X-rays at an angle of 0° or 90°, immersion of the sample in liquid nitrogen). One of the necessary conditions for obtaining high-quality measurement results, and for the subsequent creation of devices using lattice packing of SiO_2 nanospheres, is the perfection of the three-dimensional packing of nanospheres.

The obtained spectral data allow us to conclude that the radiation induced by laser irradiation at a wavelength of 1040 nm (IR), 510 nm together with 578 nm, 366 nm (UV), is low-intensity, soft X-ray radiation with a photon energy of 0.08—2.47 keV and with a wavelength of 15.2—0.5 nm. There is a reason to believe that the proper choice of the structural parameters of opal matrices (sizes of SiO_2 spherical particles, inter-sphere contact pads and monodomain regions) and characteristics of laser radiation (wavelength, pulse duration and frequency) will allow increasing the intensity and energy of X-ray quanta, which would make it possible to use the investigated effect in industry and medicine.

REFERENCES

1. Armstronga E., O'Dwyer C. Artificial opal photonic crystals and inverse opal structures — fundamentals and applications from optics to energy storage. *Journal of materials chemistry C*, 2015, vol. 3, no. 24, pp. 6109–6143, https://doi.org/10.1039/c5tc01083g

2. Samoylovich M. I., Belyanin A. F., Bagdasaryan A. S., Bovtun V. Structure and dielectric properties of nanocomposites: opal matrix – titanium oxide and rare-earth titanates. *Fine Chemical Technologies*, 2016, vol. 11, no. 2, pp. 66–73. URL: https://finechemtech.mirea.ru/upload/medialibrary/c02/09_Samoylovich_2016_No-2.pdf

3. Tuyen L. D., Wu C. Y., Anh T. K. et al. Fabrication and optical characterization of SiO_2 opal and SU-8 inverse opal photonic crystals. *Journal of Experimental Nanoscience*, 2012, vol. 7, no. 2, pp. 198–204, https://doi.org/10.1080/17458080.2010.515249

4. Miguez H., Blanco A., Lopez C. et al. Face centered cubic photonic bandgap materials based on opal-semiconductor composites. *Journal of Lightwave Technology*, 1999, vol. 17, no. 11, pp. 1975–1981, https://doi.org/10.1109/50.802983

5. Nishijima Y., Ueno K., Juodkazis S. et al. Inverse silica opal photonic crystals for optical sensing applications. *Optics Express*, 2007, vol. 15, no. 20, pp. 12979–12988, https://doi.org/10.1364/OE.15.012979

6. Sarychev A. K., Shalaev V. M. *Electrodynamics of Metamaterials*. World Scientific and Imperial College Press, 2007, 200 p., http://dx.doi.org/10.1142/4366

7. Tcherniega N. V., Samoylovich M. I., Belyanin A. F. et al. Generation of electromagnetic and acoustic emissions in nanostructures systems. *Nano- and Microsystems Technology*, 2011, no. 4, pp. 21–31. (Rus)

8. Chernega N.V. et al. *The Method of Generating Pulsed X-Ray Radiation*. Pat. 2469516 RU. 10.12.2012, bul. no. 34. (Rus)

9. Vikhlyaev D.A., Gavrilov D.S., Eliseev M.V. et al. Soft X-ray spectrometer based on spherical grazing mirrors for plasma investigation on SOKOL-P laser facility. *Problems of Atomic Science and Technology. Ser. Thermonuclear Fusion*, 2010, no. 2, pp. 57–63. URL: http://vant.iterru.ru/vant_2010_2/7.pdf (Rus)

10. Samoylovich M. I., Kleshcheva S.M., Belyanin A. F. et al. 3D-nanocomposites based on ordered packing of silica nanospheres. *Nano- and Microsystems Technology*, 2004, no. 6, pp. 3–7. (Rus)

11. Chernega N.V. et al. *Device for Generating Directional Pulsed X-Ray Radiation*. Pat. 2480159 RU. 27.04.2013, bul. no. 12. (Rus)

12. Camara C. G., Escobar J. V., Hird J. R., Putterman S. J. Sticky tape generates X rays. *Nature* 455, 2008, pp. 1089–1092. http://dx.doi.org/10.1038/news.2008.1185

Received: 08.10 2018

DOI: 10.15222/TKEA2018.5-6.10
УДК 537.9

А. Ф. БЄЛЯНІН[1], В. В. БОРИСОВ[2], В. В. ПОПОВ[3]

Росія, м. Москва, [1]ЦНДТІ «Техномаш»,
[2]НДІ ядерної фізики ім. Д. В. Скобельцина,
[3]Московський державний університет ім. М. В. Ломоносова
E-mail: belyanin@cnititm.ru

РЕНТГЕНІВСЬКЕ ВИПРОМІНЮВАННЯ, ЩО ВИКЛИКАНЕ ІМПУЛЬСНОЮ ЛАЗЕРНОЮ ДІЄЮ НА ОПАЛОВІ МАТРИЦІ

В даний час матеріали з фотонними забороненими зонами (фотонні кристали), тобто матеріали з періодичною (близько довжини хвилі світла) зміною діелектричної проникності, є об'єктом активних теоретичних та експериментальних досліджень. Для практичного застосування становлять інтерес фотонні кристали на основі опалових матриць (ОМ), які представляють собою щільну 3D-упаковку однакових за діаметром нанокуль аморфного SiO_2. Найбільший інтерес викликає застосування ОМ в малодослідженій області — генерації рентгенівського випромінювання під час лазерного впливу на речовину.

У даній роботі представлено результати вимірювання за допомогою рентгенівського спектрометра енергетичних спектрів рентгенівського випромінювання, індукованого впливом на ОМ імпульсного лазерного випромінювання з різною довжиною хвилі λ: 1040 нм (ІЧ-область спектра), 510 та 578 нм (суміщенні моди), 366 нм (УФ-область).

ОМ синтезували з розчину гідроксиду амонію (NH_4OH), етанолу (C_2H_5OH) та тетраефіра ортокремнієвої кислоти ($Si(OC_2H_5)_4$). Упаковка куль SiO_2 містила 3D-систему сполучених октаедричних і тетраедричних міжкульових пустот, які займають приблизно 26% загального об'єму. В експериментах використовували зразки ОМ в формі пластин товщиною 1–5 мм, які виготовляли за допомогою сухої механічної обробки з об'ємних ОМ, не зміцнених та зміцнених відпалом за температури 1475 К на повітрі.

Рентгенівське випромінювання, що виникає під дією лазера на ОМ, реєстрували фотоплівкою і гамма-спектрометром. Реєстрація проводилась двома способами. В першому випадку лазерне випромінювання проходило через ОМ (зйомка на просвіт) і його напрям співпадав з напрямом індукованого рентгенівського випромінювання (φ = 0°). У другому рентгенівське випромінювання проходило перпендикулярно лазерному (φ = 90°), а ОМ розміщували між пластинами з монокристалічного $LiNbO_3$. У ряді експериментів для зменшення теплового впливу на ОМ лазерного випромінювання міжкульові пустоти заповнювали водою або занурювали зразки у рідкий азот.

За результатами спектральних досліджень було встановлено, що індуковане рентгенівське випромінювання є малоінтенсивним м'яким рентгенівським випромінюванням з енергією квантів 0,08–2,47 кеВ і довжиною хвиль λ_{PI} = 15,2–0,5 нм. Спектр рентгенівського випромінювання за λ = 355 нм показав наявність додаткового, більш короткохвильового піка λ_{PI} = 1,2 нм в порівнянні з λ_{PI} = 15,2 нм, отриманим за λ = 1040 нм. Ще більш короткохвильовий пік λ_{PI} = 0,5 нм спостерігався за використання лазерного джерела, що працює з суміщеними випромінюваннями з λ = 510 нм і λ = 578 нм. Вплив на ОМ лазерного випромінювання з λ = 1040 нм призводить до сильнішого розсіювання індукованого рентгенівського випромінювання порівняно з λ = 355 нм. Вплив на ОМ лазерного випромінювання УФ-області викликав інтенсивну люмінесценцію ОМ в діапазоні видимого світла.

Показано, що на параметри рентгенівського випромінювання впливають умови отримання і ступінь заповнення пустот опалових матриць, а також умови проведення експериментів (кут отримання рентгенівського випромінювання по відношенню до лазерного, занурювання зразка у рідкий азот).

Ключові слова: опалові матриці, лазерне випромінювання, рентгенівське випромінювання, енергетичний спектр.

А. Ф. БЕЛЯНИН[1], В. В. БОРИСОВ[2], В. В. ПОПОВ[3]

Россия, г. Москва, [1]ЦНИТИ «Техномаш»,
[2]НИИ ядерной физики им. Д. В. Скобельцына,
[3]Московский государственный университет им. М. В. Ломоносова
E-mail: belyanin@cnititm.ru

РЕНТГЕНОВСКОЕ ИЗЛУЧЕНИЕ, ВЫЗВАННОЕ ИМПУЛЬСНЫМ ЛАЗЕРНЫМ ВОЗДЕЙСТВИЕМ НА ОПАЛОВЫЕ МАТРИЦЫ

В настоящее время материалы с фотонными запрещенными зонами (фотонные кристаллы), т. е. материалы с периодическим (порядка длины волны света) изменением диэлектрической проницаемости, являются объектом активных теоретических и экспериментальных исследований. Для практического применения интересны фотонные кристаллы на основе опаловых матриц (ОМ), которые представляют собой плотнейшую 3D-упаковку одинаковых по диаметру наношаров аморфного SiO_2. Наибольший интерес вызывает применение ОМ в малоисследованной области — генерации рентгеновского излучения при лазерном воздействии на вещество.

В настоящей работе представлены результаты исследования с помощью рентгеновского спектрометра энергетических спектров рентгеновского излучения, индуцированного воздействием на опаловые матрицы импульсного лазерного излучения с различной длиной волны λ: 1040 нм (ИК-область спектра), 510 и 578 нм (совмещенные моды) и 366 нм (УФ-область).

ОМ синтезировали из раствора гидрооксида аммония (NH_4OH), этанола (C_2H_5OH) и тетраэфира ортокремниевой кислоты ($Si(OC_2H_5)_4$). Упаковка шаров SiO_2 содержала 3D-систему сообщающихся октаэдрических и тетраэдрических межшаровых пустот, занимающих примерно 26% общего объема. Образцы для исследований представляли собой пластины толщиной 1,5—5,0 мм, которые получали с помощью сухой механической обработки из объемных ОМ, не упрочненных и упрочненных при отжиге до 1475 К на воздухе.

Рентгеновское излучение, возникающее при лазерном воздействии на ОМ, регистрировали фотопленкой и гамма-спектрометром. Регистрация проводилась двумя способами. В первом случае лазерное излучение проходило через ОМ (съемка на просвет) и его направление совпадало с направлением индуцированного рентгеновского излучения ($\varphi = 0°$). Во втором регистрируемое рентгеновское излучение было перпендикулярно лазерному ($\varphi = 90°$), а ОМ размещали между пластинами из монокристаллического $LiNbO_3$. В ряде экспериментов для уменьшения теплового воздействия на ОМ от лазерного излучения межшаровые пустоты заполняли водой или же погружали образцы в жидкий азот.

По результатам спектральных исследований было установлено, что индуцированное рентгеновское излучение является малоинтенсивным мягким рентгеновским излучением с энергией квантов 0,08—2,47 кэВ и с длиной волн $\lambda_{РИ}$ = 15,2—0,5 нм.

Спектр рентгеновского излучения при λ = 355 нм показал наличие дополнительного более коротковолнового пика $\lambda_{РИ}$ = 1,2 нм по сравнению с $\lambda_{РИ}$ = 15,2 нм, полученном при λ = 1040 нм. Еще более коротковолновой пик $\lambda_{РИ}$ = 0,5 нм наблюдался при использовании лазерного источника, работающего с совмещенными излучениями с λ = 510 нм и λ = 578 нм.

При воздействии на ОМ лазерного излучения с λ = 1040 нм индуцированное рентгеновское излучение рассеивалось сильнее, чем при λ = 355 нм. Воздействие на ОМ лазерного излучения УФ-области вызывало интенсивную люминесценцию ОМ в диапазоне видимого света.

Показано, что на параметры рентгеновского излучения влияют условия получения и степень заполнения пустот опаловых матриц, а также условия проведения экспериментов (угол получения рентгеновского излучения по отношению к лазерному, погружение образца в жидкий азот).

Ключевые слова: опаловые матрицы, лазерное излучение, рентгеновское излучение, энергетический спектр.

Cite the article as:
Belyanin A. F., Borisov V. V., Popov V. V. X-ray radiation during pulsed laser treatment of opal matrices. Tekhnologiya i Konstruirovanie v Elektronnoi Apparature, 2018, no. 5-6, pp. 10-16. http://dx.doi.org/10.15222/TKEA2018.5-6.10